

## Anomalies in optical harmonic generation using high-intensity laser radiation

Michelle S. Malcuit,\* Robert W. Boyd, William V. Davis,<sup>†</sup> and Kazimierz Rzażewski<sup>‡</sup>  
*Institute of Optics, University of Rochester, Rochester, New York 14627*

(Received 28 August 1989)

We observe experimentally and explain theoretically second- and third-harmonic generation from a cell containing xenon gas using a tightly focused laser beam with intensities of up to  $4 \times 10^{13}$  W/cm<sup>2</sup>. Both processes are forbidden according to standard lowest-order theories.

### INTRODUCTION

There is currently great interest in the interaction of atomic systems with extremely intense laser light. For laser intensities of the order of  $10^{13}$  W/cm<sup>2</sup> and higher, this interaction cannot be described adequately using perturbation theory. For example, above threshold ionization<sup>1</sup> (ATI, a process in which an atom absorbs more than the minimum number of photons required to become ionized) displays many features that cannot be understood by perturbative reasoning. The occurrence of ATI suggests that parametric nonlinear optical processes may also show qualitatively different features when excited using high laser intensities.<sup>2,3</sup> In fact, Li *et al.*<sup>4</sup> have observed the generation of odd harmonics of the laser frequency up to the 33rd harmonic under strong-field excitation of argon.

In this paper, we describe the results of an experimental study of harmonic generation in xenon under conditions of high-intensity excitation. Our results are somewhat unexpected. First, we observe radiation emitted in the near-forward direction at the second harmonic of our input laser frequency. Second-harmonic generation (SHG) in an isotropic medium is forbidden in the electric-dipole approximation. We present evidence that SHG is observed in our experiment due to the breaking of the inversion symmetry of the medium by the static electric field created as a result of charge separation following photoionization. This mechanism was one of those proposed by Bethune<sup>5</sup> in an attempt to explain the observation of SHG in sodium vapor.<sup>6,7</sup> However, complete agreement between theory and experiment was never obtained for the case of sodium.<sup>8</sup>

In addition, we have observed third-harmonic generation (THG) in xenon using a tightly focused laser beam and find that the intensity of the third-harmonic signal scales as the fifth power of the laser intensity. Our observations are in agreement with those of L'Huillier *et al.*<sup>9</sup> and Ganev *et al.*<sup>10</sup> These observations are somewhat surprising, firstly because the intensity of THG usually scales as the third power of the laser intensity and secondly because THG is known to be forbidden in a positively dispersive medium for tightly focused laser beams.<sup>11,12</sup> We have developed a theoretical model which shows how the modification of the propagation laws of Gaussian laser beams due to the nonlinear refractive index of the xenon gas leads to THG with an intensity that scales as the fifth power of the laser intensity.

### SECOND-HARMONIC GENERATION

Our experiment entails focusing the output of a Nd:YAG laser operating at a wavelength of  $1.06 \mu\text{m}$  and producing pulses with a duration of 30 ps and a maximum energy of 10 mJ into a cell containing up to 100 Torr of xenon gas. For peak laser intensities greater than  $1 \times 10^{13}$  W/cm<sup>2</sup> we observed SHG emitted in the near-forward direction. Figure 1 shows the far-field intensity distribution of the second-harmonic radiation both for linear [1(a)–1(c)] and circular [1(d)] polarizations of the fundamental laser beam. Figure 2(a) shows that the intensity of the second-harmonic signal scales approximately as the 13th power of the fundamental laser intensity  $I$  when the xenon pressure  $p_{\text{Xe}}$  is held fixed at 15 Torr. Figure 2(b) shows that the intensity of the second-harmonic signal scales as the third power of  $p_{\text{Xe}}$  when the laser intensity is held fixed at  $4 \times 10^{13}$  W/cm<sup>2</sup>. These observations are explained by the following model.

SHG by a phase-matched process is forbidden in the electric-dipole approximation for materials possessing inversion symmetry. A number of physical mechanisms which can break the inversion symmetry of an atomic gas and lead to SHG have been described by Bethune.<sup>5</sup> We find that only one of the proposed mechanisms is consistent with our experimental results. According to this mechanism, the inversion symmetry of the medium is broken by a cylindrically symmetric static electric field which results from charge separation following photoionization. We assume that  $N_i$  ions per unit volume are thereby created, and that the photoelectrons are ejected with average kinetic energy  $T$ . The electrons are ejected mostly along the polarization direction of the laser light.<sup>13</sup> However, the spatial distribution of the electrons rapidly equilibrates and creates a cylindrically symmetric electron cloud surrounding a region containing the positive ions. The characteristic time for this equilibration to occur is the inverse of the plasma frequency  $\omega_p = (4\pi N_e e^2/m)^{1/2}$ , which, assuming 1% ionization of the xenon gas, leads to a time  $\tau_p$  of 300 fs, which is much shorter than the duration of our laser pulse. We can estimate the magnitude of the static electric field created by this charge distribution by equating the total kinetic energy of the ejected electrons  $N_i TV$  (where  $V$  is the interaction volume) with the energy stored in the static electric field  $E_0^2 V/8\pi$ , to obtain the result  $E_0 = (8\pi N_i T)^{1/2}$ . We estimate the kinetic energy  $T$  as  $S\hbar\omega$ , where due to the effects of ATI (Ref. 1) the parameter  $S$  is of the order of

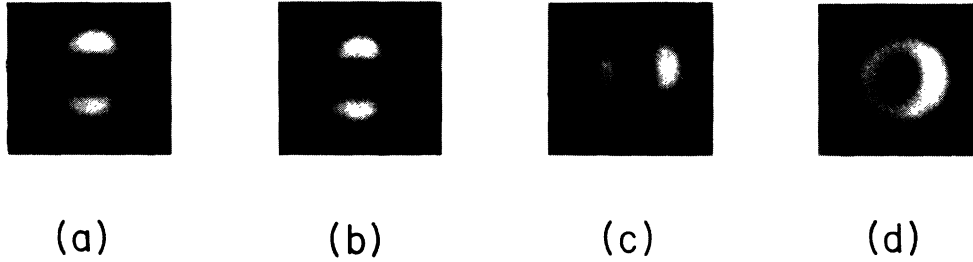


FIG. 1. Far-field intensity distributions of the second-harmonic generation (SHG) with the fundamental laser beam polarized linear and vertical (a)–(c) and circular (d). (a) shows the distribution of the total emitted radiation, (b) shows the distribution of the vertically polarized radiation, and (c) shows the distribution of the horizontally polarized radiation. Photograph (c) has been exposed for nine times longer than photographs (a) and (b). For a circularly polarized laser beam, the SHG is emitted in a ring (d) with the same circular polarization as the fundamental.

5. Again assuming 1% ionization, so that  $N_i = 5.3 \times 10^{15} \text{ cm}^{-3}$ , we find that  $E_0 = 1000 \text{ statvolt/cm}$ . The ponderomotive force can also lead to a charge separation which would break the inversion symmetry. However, for our laser intensity of  $4 \times 10^{13} \text{ W/cm}^2$ , the electric field created in response to the ponderomotive potential energy  $e^2|E_1|^2/m\omega^2$  is only of the order of 2 statvolt/cm. Hence under our experimental conditions ponderomotive effects play essentially no role.

Due to the presence of the static field  $E_0$ , SHG can occur in a nominally isotropic medium. The nonlinear polarization leading to SHG can be expressed as

$$\mathbf{P}_2 = \chi_a^{(3)}(\mathbf{E}_0 \cdot \mathbf{E}_1)\mathbf{E}_1 + \chi_b^{(3)}(\mathbf{E}_1 \cdot \mathbf{E}_1)\mathbf{E}_0, \quad (1)$$

where  $\chi_a^{(3)}$  and  $\chi_b^{(3)}$  are the two independent components of the nonlinear susceptibility tensor. In general,  $\chi_a^{(3)}$  and  $\chi_b^{(3)}$  depend differently<sup>5</sup> on the laser frequency  $\omega$ . However, under our experimental conditions of nonresonant excitation, the ratio  $\chi_b^{(3)}/\chi_a^{(3)}$  approaches the limiting value of  $\frac{1}{2}$ . Equation (1) explains fully the observed polarization and spatial distributions of the generated radiation shown in Fig. 1. Since the static electric field vanishes on axis and peaks near the edge of the laser beam, the nonlinear polarization  $\mathbf{P}_2$  also vanishes on axis. This polarization will tend to radiate a second-harmonic field in the

form of a (generally nonaxially symmetric) cone. For the case of a linearly polarized laser beam, Eq. (1) with  $\chi_b^{(3)}/\chi_a^{(3)} = \frac{1}{2}$  predicts that 90% of the power of the emitted radiation will be polarized parallel to the polarization of the incident laser beam and 10% will be emitted in the orthogonal polarization. Each polarization component is emitted in a double-lobed pattern with the lobes separated along the direction of polarization. For the case of a circularly polarized laser beam, the second term in Eq. (1) vanishes, and the second-harmonic radiation is emitted in the form of a uniform cone with the same polarization as the laser.

The observed  $I^{13}$  and  $p_{\text{Xe}}^3$  dependences of the intensity of the second-harmonic radiation are also in agreement with the predictions of this model. The static field  $E_0$  which appears in Eq. (1) is proportional to  $N_i^{1/2}$ , and in the perturbation theory limit  $N_i$  is proportional to the product of the xenon pressure and the 11th power of the laser intensity because 11 photons are required to ionize xenon. Hence  $\mathbf{P}_2$  is proportional to  $E_1^{13}$ , which explains the laser intensity dependence of the second-harmonic signal. In addition, since  $\mathbf{P}_2$  is proportional to  $N_a E_0$  where  $N_a$  is proportional to  $p_{\text{Xe}}$  and where  $E_0$  is proportional to  $p_{\text{Xe}}^{1/2}$ , the second-harmonic intensity is predicted to be proportional to the third power of the xenon pressure.

The efficiency of conversion of fundamental photons into second-harmonic photons for a linearly polarized fundamental beam is measured to be  $\eta_2 \approx 2 \times 10^{-11}$  to within a factor of 3. We estimate the conversion efficiency assuming plane-wave propagation and perfect phase matching as  $\eta_2 = 9\pi^3 k_1^2 (\chi^{(3)})^2 I E_0^2 b^2 / c$  where  $\chi^{(3)}$  is the nonlinear susceptibility,  $k_1$  is the wave number of the fundamental radiation,  $w_0$  is the beam waist radius, and  $b = k_1 w_0^2$  is the characteristic diffraction length of the laser beam. Under our experimental conditions, the maximum pulse energy was 10 mJ and the pulse shape was nearly Gaussian with a full width at half maximum (FWHM) duration of 30 ps. We determine  $\chi^{(3)} = N_a \gamma$  using  $N_a = 5.3 \times 10^{17} \text{ cm}^{-3}$  at 15 Torr and  $\gamma = 9 \times 10^{-37} \text{ esu}^{11}$  as  $\chi^{(3)} = 4.8 \times 10^{-19} \text{ esu}$ . We thereby find that  $\eta_2 = 1 \times 10^{-11}$ , in good order-of-magnitude agreement with our experimental results.

Two other mechanisms that have been proposed<sup>5</sup> as

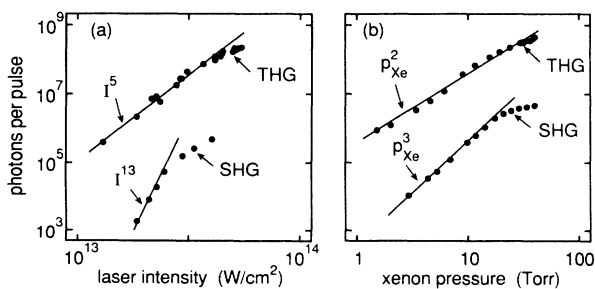


FIG. 2. Number of emitted photons for second-harmonic generation (SHG) and third-harmonic generation (THG) (a) plotted vs laser intensity  $I$  with the xenon pressure held fixed at 15 Torr and (b) plotted vs xenon pressure  $p_{\text{Xe}}$  with the laser intensity held fixed at  $4 \times 10^{13} \text{ W/cm}^2$ . The straight lines show the various functional dependences.

the origin of SHG in atomic gases are generation by higher-order multipoles and radiation by nonuniformly distributed free electrons. Under our experimental conditions, both processes lead to a much smaller conversion efficiency and to a pressure dependence different from that measured experimentally.

### THIRD-HARMONIC GENERATION

We have also studied the properties of the THG process. We find that the third-harmonic radiation is generated on axis with a far-field spot size approximately equal to that of the fundamental laser beam. Figure 2(b) shows that the intensity of the third-harmonic radiation scales as the square of the xenon pressure (for a laser intensity of  $4 \times 10^{13}$  W/cm<sup>2</sup>) as expected for a phase-matched nonlinear optical process driven by a prescribed optical field in the low conversion efficiency limit. Figure 2(a) shows that, with the xenon pressure held fixed at 15 Torr, the intensity of the third-harmonic signal scales as the fifth power of the laser intensity. We have developed the following theoretical model to explain this anomalous dependence on the laser intensity. It is well known that no THG is produced for a tightly focused Gaussian laser beam for the case in which the wave-vector mismatch  $\Delta k = 3k_1 - k_3$  is negative,<sup>11,12</sup> as it was in our experiment. (We estimate that  $b\Delta k = -0.01$  for our experimental conditions.) We believe that THG occurred in our experiment due to a modification of the propagation of the fields by the nonlinearity of the refractive index of the xenon gas.<sup>14</sup> We do not believe that plasma generation is important in producing THG because we observe an  $I^5$  dependence, whereas 11 photons are required to ionize xenon. To describe the propagation of a Gaussian laser beam through a nonlinear medium, we make use of the aberrationless approximation,<sup>15</sup> which assumes that the laser beam remains Gaussian but with a spot size  $w(z)$  and phase  $\psi(z)$  that vary with  $z$  in a manner different from that predicted by the usual law for propagation through a linear medium. We consider the propagation of a Gaussian laser beam of field strength  $A_1(r,z) \exp(ik_1z - i\omega t) + \text{c.c.}$  through a medium with a third-order nonlinearity. We perform a calculation similar to that described by Akhmanov *et al.*<sup>15</sup> who considered only the amplitude but not the phase of the beam. We introduce the dimensionless coordinate  $\xi = 2z/b$  and the parameter  $\beta = 6\pi\chi^{(3)}|E_1|^2(k_1w_0)^2$  that characterizes the strength of the nonlinearity. We find that the propagation of the laser beam is described for  $\beta < 1$  by

$$A_1(r,z) = \frac{E_1}{[(1-\beta) + \xi^2]^{1/2}} \times \exp\left[-\frac{r^2(1-i\xi)}{w_0^2[(1-\beta) + \xi^2]}\right] \exp[-i\psi(\xi)] \quad (2a)$$

where

$$\psi(\xi) = \frac{1-\beta/2}{\sqrt{1-\beta}} \tan^{-1}\left[\frac{\xi}{\sqrt{1-\beta}}\right]. \quad (2b)$$

Note that the parameter  $\beta$  depends on the power  $P$  carried by the beam (rather than the intensity) and can be identified with the ratio  $P/P_{cr}$ , where  $P_{cr}$  is the minimum power required for self-focusing to occur. Under our experimental conditions,  $\beta$  is equal to  $8 \times 10^{-3}$  at the peak of the laser pulse. Since  $\beta$  is much smaller than unity, essentially no modification of the intensity distribution of the beam occurs; the primary influence of the nonlinear refractive index is to produce changes in the phases of the interacting fields. We show below that these phase shifts lead to THG with an intensity that scales as the fifth power of the laser intensity.

We describe the generation of the third-harmonic field through use of the paraxial wave equation for the third-harmonic field amplitude  $A_3$ :

$$2ik_3 \frac{\partial A_3}{\partial z} + \nabla_T^2 A_3 = -4\pi\chi^{(3)}k_3^2 A_1^3 e^{i\Delta kz} - 24\pi\chi^{(3)}k_3^2 |A_1|^2 A_3, \quad (3)$$

where the two source terms describe the direct generation of the third-harmonic field and the nonlinear modification of the propagation of the third-harmonic field, respectively. We have been unable to solve Eq. (3) with  $A_1$  given by Eq. (2). We therefore seek an approximate solution to Eq. (3) in the form of a Gaussian laser beam

$$A_3(r,z) = \frac{E_3(z)}{1+i\xi} \exp\left[-\frac{3r^2}{w_0^2(1+i\xi)}\right]. \quad (4)$$

We solve for the unknown function  $E_3(z)$  by a perturbation expansion. We first expand the source term  $A_1(r,z)$  in a power series in the small parameter  $\beta$ . We find, in the aberrationless approximation (i.e., ignoring corrections to the Gaussian radial dependence), that  $A_1(r,z)$  is given by

$$A_1(r,z) = \frac{E_1}{1+i\xi} \exp\left[-\frac{r^2}{w_0^2(1+i\xi)}\right] \times \left[1 + \frac{\beta}{2(1+i\xi)} + \dots\right]. \quad (5)$$

To lowest order in our perturbation expansion (i.e., first order in  $\beta$ ), we omit the second term on the right-hand side of Eq. (3) and replace  $A_1$  by  $A_1^{(0)}$ , its unmodified value, obtained by setting  $\beta$  equal to zero in Eq. (2). We find that the first-order contribution to  $E_3(z)$  is given by

$$E_3^{(1)}(z) = \frac{i\beta E_1}{2} \int_{-\infty}^{\xi} d\xi' \frac{e^{i(1/2)b\Delta k\xi'}}{(1+i\xi')^2}. \quad (6)$$

The integral is readily evaluated in the limit  $\xi \rightarrow \infty$ , and we obtain the well-known result that  $E_3^{(1)}$  vanishes for  $\Delta k \leq 0$ . Hence, in lowest order, no THG occurs under our experimental conditions.

In the next order of approximation (i.e., second order in  $\beta$ ), both source terms of Eq. (3) are present. The first term is of the form

$$[-6\pi k_3^2 \beta \chi^{(3)} (A_1^{(0)})^3 \exp(i\Delta kz)] / (1+i\xi).$$

However, this source term does not lead to THG as  $z \rightarrow \infty$  either, as one can show by means of a calculation analogous to that of Eqs. (4) and (6). The second source term is of the form  $-24\pi k_3^2 \chi^{(3)} |A_1^{(0)}|^2 A_3^{(1)}$  where  $A_3^{(1)}(r, z)$  is given by Eq. (4) with  $E_3(z)$  replaced by expression (6) for  $E_3^{(1)}(z)$ . We find that for this source term the wave equation is satisfied (to lowest order in  $r/w_0$ ) for  $E_3^{(2)}(z)$  given by

$$E_3^{(2)}(z) = \frac{-3\beta^2 E_1}{2} \int_{-\infty}^{\xi} \frac{d\xi'}{1+\xi'^2} \int_{-\infty}^{\xi'} \frac{e^{i(1/2)b\Delta k \xi''}}{(1+i\xi''')^2} d\xi'''. \quad (7)$$

For  $\Delta k = 0$  and  $z \rightarrow \infty$ , we find that  $E_3^{(2)} = -i\frac{3}{4}\pi\beta^2 E_1$ . Since  $\beta$  is proportional to  $|E_1|^2$ , Eq. (7) predicts that the third-harmonic intensity will be proportional to the fifth power of the laser intensity, as observed in our experiment. The maximum experimentally observed photon conversion efficiency  $\eta_3$  was equal to  $\sim 2 \times 10^{-9}$ . The theoretically predicted conversion efficiency is obtained by integrating the predicted third-harmonic intensity over the temporal and spatial distributions of the laser

pulse. We find that  $\eta_3 = 1 \times 10^{-9}$ , which is within a factor of 2 different of the observed value.

## CONCLUSIONS

In conclusion, we have observed second- and third-harmonic generation in xenon gas under conditions where naive theories predict that these effects should not occur, and we have developed theoretical models that explain these observations. Similarly, higher-order effects are expected to influence the generation of all higher-order harmonics, complicating the relation between the nonlinear response of individual atoms and the optical signal observed from extended samples.

## ACKNOWLEDGMENTS

This work was supported by the National Science Foundation and the U. S. Army Research Office, University Research Initiative.

\*Present address: Department of Physics, Lehigh University, Bethlehem, Pennsylvania 18015.

†W. V. Davis is also with the Department of Physics, University of Rochester, Rochester, New York 14627.

‡Permanent address: Institute for Theoretical Physics, Polish Academy of Sciences, 02668 Warsaw, Poland.

<sup>1</sup>P. Kruit, J. Kimman, H. G. Muller, and M. J. van der Wiel, *Phys. Rev. A* **28**, 248 (1983); for a recent review of strong-field ionization see P. Agostini and G. Petite, *Contemp. Phys.* **29**, 57 (1988).

<sup>2</sup>C. K. Rhodes, *Phys. Scr.* **T17**, 193 (1987); M. Ferray, A. L'Huillier, X. F. Li, L. A. Lompré, G. Mainfray, and C. Manus, *J. Phys. B* **21**, L 31 (1988).

<sup>3</sup>B. W. Shore and P. L. Knight, *J. Phys. B* **20**, 413 (1987); K. C. Kulander and B. W. Shore, *Phys. Rev. Lett.* **62**, 524 (1989); J. H. Eberly, Q. Su, and J. Javanainen, *ibid.* **62**, 881 (1989).

<sup>4</sup>X. F. Li, A. L'Huillier, M. Ferray, L. A. Lompré, and G. Mainfray, *Phys. Rev. A* **39**, 5751 (1989).

<sup>5</sup>D. S. Bethune, *Phys. Rev. A* **23**, 3139 (1981).

<sup>6</sup>T. Mossberg, A. Flusberg, and S. R. Hartmann, *Opt. Commun.* **25**, 121 (1978); R. R. Freeman, J. E. Bjorkholm, R. Panock, and W. E. Cooke, in *Laser Spectroscopy V*, edited by A. R. W. McKeller, T. Oka, and B. P. Stoicheff (Springer-Verlag, New York, 1981), p. 453.

<sup>7</sup>K. Miyazaki, T. Sato, and H. Kashiwagi, *Phys. Rev. Lett.* **43**, 1154 (1979).

<sup>8</sup>Bethune's model (Ref. 5), while internally consistent, was never fully accepted as the explanation of SHG in sodium vapor because of disagreements between the predictions of the model and published experimental results. The most significant

discrepancy is that the model predicts an  $N_a^3$  dependence of the second-harmonic intensity on atomic number density  $N_a$ , whereas the experimental results reported by Miyazaki *et al.* showed an  $N_a^2$  dependence. However, we have repeated their experiment and find the  $N_a^3$  dependence predicted by the model. Also, the predictions of Bethune's model for the polarization properties of SHG depend critically upon the detuning of the laser from resonance. Under the experimental conditions of Miyazaki *et al.*, the detuning of the laser from the atomic resonance and the optical Stark shifts of the interacting levels are of the same order of magnitude, which greatly complicates the theoretical analysis of the experiment. This effect is negligible under our experimental conditions of highly nonresonant excitation.

<sup>9</sup>A. L'Huillier, L. A. Lompré, M. Ferray, X. F. Li, G. Mainfray, and C. Manus, *Europhys. Lett.* **5**, 601 (1988).

<sup>10</sup>R. Ganeev, V. Gorbushin, I. Kulagin, and T. Usmanov, *Opt. Spectrosc.* **61**, 807 (1986).

<sup>11</sup>J. F. Ward and G. H. C. New, *Phys. Rev.* **185**, 57 (1969).

<sup>12</sup>R. B. Miles, and S. E. Harris, *IEEE J. Quantum Electron.* **QE-9**, 470 (1973); G. C. Bjorklund, *ibid.* **QE-11**, 287 (1975).

<sup>13</sup>H. J. Humpert, H. Schwier, R. Hippler, and H. O. Lutz, *Phys. Rev. A* **32**, 3787 (1985).

<sup>14</sup>R. Rosman, G. Gibson, H. Jara, T. S. Luk, I. A. McIntyre, A. McPherson, J. C. Solem, and C. K. Rhodes, *J. Opt. Soc. Am. B* **5**, 1237 (1988).

<sup>15</sup>S. A. Akhmanov, R. V. Khokhlov, and A. P. Sukhorukov, in *Laser Handbook II*, edited by F. T. Arrechi and E. O. Schulz-Dubois (North-Holland, Amsterdam, 1972).

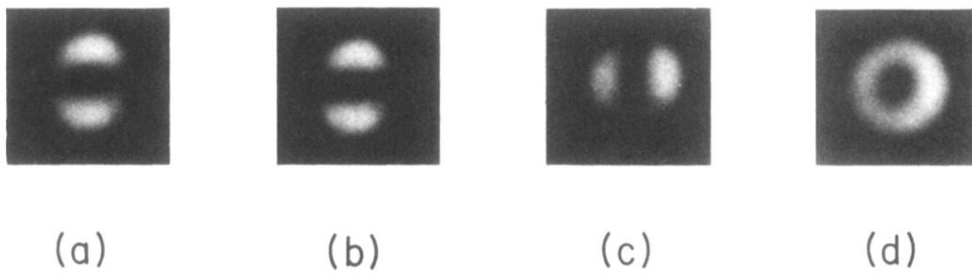


FIG. 1. Far-field intensity distributions of the second-harmonic generation (SHG) with the fundamental laser beam polarized linear and vertical (a)–(c) and circular (d). (a) shows the distribution of the total emitted radiation, (b) shows the distribution of the vertically polarized radiation, and (c) shows the distribution of the horizontally polarized radiation. Photograph (c) has been exposed for nine times longer than photographs (a) and (b). For a circularly polarized laser beam, the SHG is emitted in a ring (d) with the same circular polarization as the fundamental.